water

MDPI

Article

Evaluation of the Artificial Neural Networks—Dynamic Infrared Rain Rate near Real-Time (PDIR-Now) Satellite's Ability to Monitor Annual Maximum Daily Precipitation in Mainland China

Yanping Zhu [1], Gaosong Chang [2], Wenjiang Zhang [1], Jingyu Guo [3] and Xiaodong Li [1,4,*]

[1] State Key Laboratory of Hydraulics and Mountain River Engineering & College of Water Resource and Hydropower, Sichuan University, Chengdu 610065, China; zhuyanping@stu.scu.edu.cn (Y.Z.); zhang_wj@scu.edu.cn (W.Z.)
[2] Sichuan Hydrology and Water Resources Survey Center, Chengdu 638404, China; changgaosongdra@163.com
[3] Sichuan China Railway Erju Engineering Group Co., Ltd., Chengdu 610213, China; guojingyu999@163.com
[4] Tianfu Yongxing Laboratory, Chengdu 610213, China
* Correspondence: lxdscu@163.com; Tel.: +86-138-8072-5943

Abstract: As one of the countries with the most severe extreme climate disasters in the world, it is of great significance for China to scientifically understand the characteristics of extreme precipitation. The artificial neural network near-real-time dynamic infrared rainfall rate satellite precipitation data (PDIR-Now) is a global, long-term resource with diverse spatial resolutions, rich temporal scales, and broad spatiotemporal coverage, providing an important data source for the study of extreme precipitation. But its applicability and accuracy still need to be evaluated in specific applications. Based on the observation data of 824 surface meteorological stations in China, the correlation coefficient (*R*), relative deviation (*RB*), root mean square error (*RMSE*), and relative root mean square error (*RRMSE*) of quantitative statistical indicators were used to evaluate the annual maximum daily precipitation of PDIR-Now from 2000 to 2016 in this study, in order to explore the ability of PDIR-Now satellite precipitation products to monitor extreme precipitation in Chinese mainland. The results show that from the perspective of long-term series, the annual maximum daily precipitation of PDIR-Now has a good ability to monitor extreme precipitation across the country, and the *R* exceeds 0.6 in 65% of the years. The *RMSE* of different years is generally distributed between 40 and 60 mm, and in terms of time characteristics, the error of each year is relatively stable and does not fluctuate greatly with dry precipitation or abundant years. From the perspective of spatial characteristics, the distribution of *RMSE* is very regional, with the *RMSE* in the Qinghai–Tibet Plateau and Northwest China basically in the range of 0~20 mm, the Yunnan–Guizhou Plateau, the Sichuan Basin, Northeast China, and the central part of the study area in the range of 20~50 mm, and the *RMSE* in a few stations in the southeast coast greater than 80 mm. The *RRMSE* distribution of most sites is between 0 and 0.6, and the *RRMSE* distribution of a few sites is between 0.6 and 1.5. Generally, higher *RRMSE* values and larger errors are observed in the northwest and southeast coastal regions. Overall, PDIR-Now captures the regional characteristics of extreme precipitation in the study area, but it is underestimated in the wet season in humid and semi-humid regions and overestimated in the dry season in arid and semi-arid regions.

Keywords: PDIR-Now satellite; extreme precipitation; accuracy evaluation; China

Academic Editor: Paul Kucera

Received: 5 December 2024
Revised: 15 January 2025
Accepted: 16 January 2025
Published: 23 January 2025

Citation: Zhu, Y.; Chang, G.; Zhang, W.; Guo, J.; Li, X. Evaluation of the Artificial Neural Networks—Dynamic Infrared Rain Rate near Real-Time (PDIR-Now) Satellite's Ability to Monitor Annual Maximum Daily Precipitation in Mainland China. *Water* **2025**, *17*, 308. https://doi.org/10.3390/w17030308

1. Introduction

The annual maximum daily precipitation (AMDP) dataset is one of the most important and easily accessible metrics for studying extreme rainfall, and it holds significant value in fields such as meteorology, hydrology, and disaster management. This metric is determined by observing daily precipitation data over the course of a year and identifying the day with the highest precipitation. Typically, these data are collected from meteorological stations, rain gauges, and satellite monitoring systems. Through long-term observation and data recording, extreme precipitation events in different years and regions can be analyzed and compared, providing essential data support for climate change research, flood, debris flow, and landslide risk assessments, water conservancy project planning and management, and urban planning and management [1–3].

Satellite precipitation monitoring datasets offer long-term estimates of climate variables that cover either the globe or specific regions. Using satellite data for monitoring the annual maximum daily precipitation has important significance in both scientific research and practical applications. Satellite monitoring technology employs passive microwave and active radar methods to acquire precipitation information, which is then processed and corrected through complex algorithms to provide globally covered, high temporal and spatial resolution, long-term continuous precipitation data [4–6]. This not only helps scientists to gain a deeper understanding of precipitation processes and the impacts of climate change but also provides valuable data support to various sectors in responding to extreme precipitation events [7–10].

However, satellite precipitation products are indirect measurements and contain errors relative to actual precipitation, so they must be assessed for accuracy and applicability before use. Many studies, both domestic and international, have focused on evaluating the ability of satellite data to monitor annual maximum daily precipitation. Internationally, many researchers have used satellite data from missions such as TRMM (Tropical Rainfall Measuring Mission) and GPM (Global Precipitation Measurement) to conduct such evaluations with significant results. For example, Huffman et al. (2010) studied the application of TRMM data in global precipitation estimation and highlighted its high accuracy in tropical and subtropical regions [11]. Skofronick-Jackson et al. (2017) evaluated the precipitation observation capability of the GPM satellite and validated its effectiveness in monitoring extreme precipitation events [12]. Echeta, O.C. et al. (2022) assessed four near-real-time satellite precipitation products (GSMaP_NRT, IMERG-E, PERSIANN-CCS, and PDIR-Now) in the Volta Basin and compared them with real-time, post-satellite precipitation products. The results indicated that PDIR-Now had the highest probability of detecting extreme rainfall among all the products [13]. Vesta Afzali Gorooh et al. (2022) conducted a study on PDIR-Now along the Pacific coast of the United States, focusing on complex topography. The results showed that this satellite product performed more accurately in detecting precipitation events in cold bright bands (BBs) and warmer non-bright bands (NBBs) in topologically complex regions [14]. Alharbi R.S. et al. (2024) evaluated the daily precipitation and four extreme precipitation indices of the PDIR-Now satellite product in Saudi Arabia using six evaluation indicators. Their findings highlighted the potential of the PDIR-Now satellite product for precipitation assessment [3].

In China, researchers have also evaluated the ability of satellite precipitation to monitor extreme values. For instance, Liu et al. (2017) used multiple satellite products from the GPM era to monitor and evaluate Typhoon Rammasun in specific regions of China [15]. Liu Yu et al. (2017) used seven extreme rainfall indices to assess the performance of three major satellite precipitation products—TRMM 3B42, TRMM 3B42RT, and CMORPH—in China [16]. Pang Chenkun (2023) used thirteen representative satellite precipitation products to calculate extreme precipitation indices and evaluate their ability to monitor extreme

precipitation across different spatiotemporal scales, further exploring the spatiotemporal differences in satellite precipitation products' monitoring capabilities for extreme precipitation [17]. Although there is limited research on the precipitation extremes of the PDIR-Now satellite product in China, studies on its applicability in specific regions do exist. For example, Wan-Ru Huang et al. (2021) conducted a comparative evaluation of five PERSIANN satellite products in Taiwan and pointed out that PDIR-Now and PERSIANN-CCS-CDR had smaller RMSE than the other three satellite products at different time scales. Moreover, PDIR-Now was identified as the best product for quantitatively estimating precipitation at interannual, annual, and seasonal time scales [7]. Wenhao Xie et al. (2022) evaluated six satellite precipitation products (IMERG, CMORPH, GSMaP, PERSIANN, PERSIANN-CCS, and PDIR-Now) in the northwestern part of China. The results showed that the bias in the performance evaluation of the satellite products was significant in the study area, emphasizing the need for accurate understanding of the performance of the satellite precipitation products when using satellite data and the importance of bias correction [18].

Despite the evident importance of reliable annual maximum daily precipitation data and the numerous regional studies on its impacts [19–31], to our knowledge, there has been no study evaluating the monitoring capability of annual maximum daily precipitation using the artificial neural network near-real-time dynamic infrared rainfall rate satellite precipitation data (PDIR-Now) in this study area. PDIR-Now is an innovative, global, long-term resource that provides diverse spatial resolutions, rich temporal scales, and extensive spatiotemporal coverage, making it a valuable data source for studying extreme precipitation [25,32]. Therefore, this study takes the observed data from 824 ground meteorological stations in China as a benchmark and uses quantitative statistical indicators R (correlation coefficient), RB (relative bias), RMSE (root mean square error), and RRMSE (relative root mean square error) to evaluate the PDIR-Now annual maximum daily precipitation from 2000 to 2016, aiming to explore the ability of the PDIR-Now satellite precipitation product to monitor extreme precipitation in mainland China. The results of this study will help users to assess the accuracy of the data, enabling timely identification of the impact of precipitation products on future research. This will allow researchers to adjust their study plans, reduce errors in research, and improve the quality of experimental results. For developers of precipitation products, testing the accuracy of the data can provide timely improvements to the algorithms, facilitating the further development and promotion of these products.

2. Materials and Methods

2.1. Study Area

This study selects the territory of China and a 20 km buffer zone extending outward (Figure 1) as the study region. The longitude range is from 73°21′ E to 135°22′ E, and the latitude range is from 3°65′ N to 53°53′ N. The total area of the region is approximately 17.265 million square kilometers. The climate in this region is highly variable, with complex terrain. It encompasses tropical, subtropical, and temperate monsoon climates, as well as temperate desert, steppe climates, and alpine plateau climates. The region also includes a variety of topographies, such as plateaus, basins, mountains, hills, and plains. In addition, it has many major river systems, such as the Yangtze River, Yellow River, West River, Heilongjiang River, and Yarlung Tsangpo River, as well as glaciers and grasslands. Due to China's vast latitudinal range, the region spans several temperature zones, including the cold temperate zone, middle temperate zone, warm temperate zone, subtropical zone, tropical zone, and the unique alpine cold zone of the Tibetan Plateau. These climatic and geographical factors result in uneven spatial and temporal precipitation distributions, with distinct seasonal and latitudinal variations between the north and south.

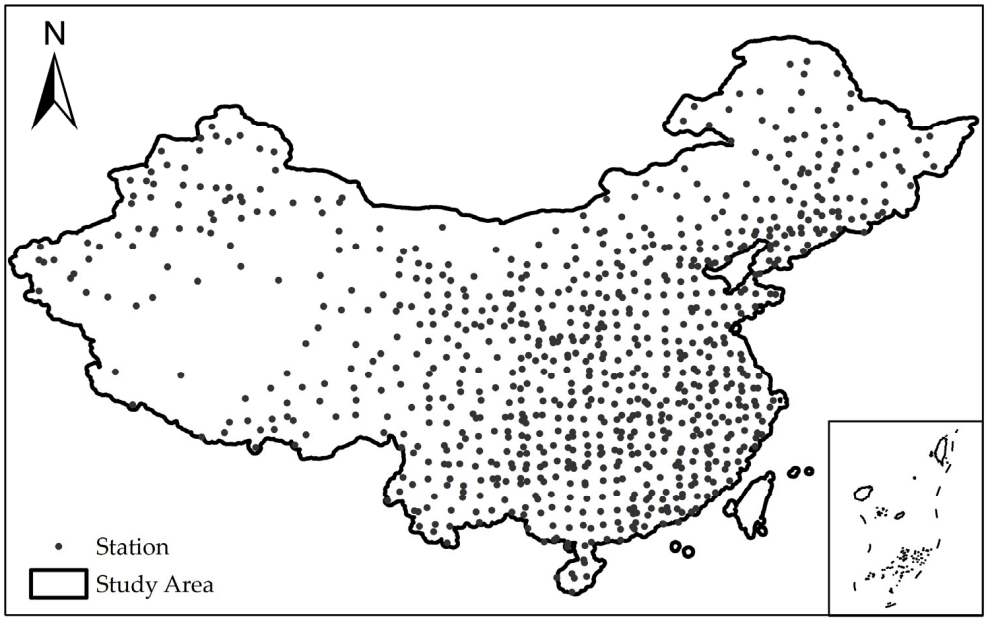

Figure 1. Study area and meteorological stations.

2.2. Data Sources

The data used in this study mainly come from two sources: the PDIR-Now satellite precipitation product data (the unverified data) and the precipitation observation data from meteorological stations in China (the standard data).

2.2.1. Station Data

In this study, 824 meteorological stations within the study area were selected, and their precipitation data were used as ground reference data. After review and quality checks, this includes the continuity of the data, removing stations with missing data, and comparing the annual precipitation values obtained by aggregating daily-scale precipitation data from the stations with the existing station annual precipitation values to eliminate stations with large errors. The final stations used in this study all have uninterrupted long-term time series data for 17 years. The corresponding satellite data for the geographical locations of the stations also meet the requirements for studying extreme values. The distribution of the stations is shown in Figure 1, and the selected meteorological stations cover as much of the study area as possible. However, due to the remote geographic location and complex terrain of the Tibetan Plateau, station observations are difficult to carry out, resulting in fewer stations. Additionally, because of the low population density and rare extreme precipitation events in the region, the stations in this area are sparsely distributed. The station data source is the Meteorological Research Center of the China Meteorological Administration. The precipitation data selected included 17 years, from 2000 to 2016. The data scale is on a daily basis, with a time span from 20:00 to the next day at 20:00. The data are measured in 0.1 mm, and the data format is TXT. To unify the scale, the original data were processed to use 1 mm as the unit of measurement.

2.2.2. PDIR-Now Satellite Product Data

The PDIR-Now precipitation data come from the real-time, global, high-resolution satellite precipitation product developed by the Hydrometeorology and Remote Sensing Center (CHRS) at the University of California, Irvine. The main advantage of PDIR-Now, compared to other near-real-time precipitation datasets, is that it relies on high-frequency

sampling of infrared images, resulting in a short delay (15–60 min). Additionally, PDIR-Now improves the errors and uncertainties associated with using infrared imagery by employing dynamic offset models based on the dynamic cloud top brightness temperature–rainfall rate (Tb-R) curve. The short delay of PDIR-Now makes this dataset particularly suitable for near-real-time hydrological applications, such as flood forecasting and the development of flood inundation maps. The PDIR-Now algorithm also has potential for reconstructing historical precipitation estimates at high temporal and spatial resolution [25,32].

In this study, the global precipitation data of the PDIR-Now remote sensing dataset from 2000 to 2016 on an hourly scale for 17 years were selected. The basic information of the dataset is as follows: temporal resolution of 1 h, with precipitation units in 1 mm; spatial resolution of 0.04°, i.e., a 4 km × 4 km grid; and the data format is TIF. Although there are missing satellite data in some years and months for the northwest and northeast regions, investigations have confirmed that the missing data do not affect the extraction of the annual maximum daily precipitation. Regarding time processing, China's time is eight hours ahead of Greenwich Mean Time (GMT+8). To match the temporal resolution of the station data, precipitation data at the hourly scale were preprocessed by summing the precipitation data from 12:00 PM of the current day to 12:00 PM of the next day. Then, grid data are extracted using the station coordinates in order to match the precipitation data from 8:00 PM of the current day to 8:00 PM of the next day in China.

2.3. Performance Evaluation Methods

To comprehensively evaluate the statistical significance of the satellite extreme precipitation and its practicality in the study area, the station data were used as the benchmark. The corresponding grid data from the PDIR-Now satellite product were extracted based on the station coordinates. Three aspects were considered for the evaluation: (1) extracting station observation data for the same period to assess the satellite's annual maximum daily precipitation, (2) extracting satellite data for the same period to assess station-based annual maximum daily precipitation, and (3) using the annual maximum value method based on flood sampling to evaluate the annual maximum daily precipitation for both datasets.

The evaluation used an inversion accuracy evaluation index system, which includes both consistency indicators and error indicators. These include the correlation coefficient (*R*), relative bias (*RB*), root mean square error (*RMSE*), and relative root mean square error (*RRMSE*) [33–36]. These performance evaluation indicators are widely applied in research on multi-satellite remote sensing precipitation products. The correlation coefficient (*R*) is a good indicator of the degree of fit between the two datasets. To determine the accuracy of the satellite's precipitation estimates for different years, this parameter was chosen as a key evaluation criterion. *RMSE* and *RB* were selected to assess the prediction accuracy, as they focus on different aspects. *RMSE* reveals the absolute error between predicted and observed values, while RB highlights the proportional difference between predicted and actual values. *RRMSE*, as an additional indicator, provides a more intuitive understanding of the regional characteristics of the errors.

The specific expressions and criteria for each metric are as follows:

(1) Correlation Coefficient (*R*)

$$R = \frac{\sum_{i=1}^{n} (S_i - \overline{S})(G_i - \overline{G})}{\sqrt{\sum_{i=1}^{n} (S_i - \overline{S})^2} \sqrt{\sum_{i=1}^{n} (G_i - \overline{G})^2}}$$

In the formula, the range of R is −1~1, and R is a positive value indicating that the two datasets are positively correlated and, vice versa, are negatively correlated.

(2) Root Mean Square Error (*RMSE*)

$$RMSE = \sqrt{\frac{1}{n}\sum_{i=1}^{n}(S_i - G_i)^2}$$

In the formula, the range of *RMSE* is 0~∞, and there is no difference at 0.

(3) Relative Root Mean Square Error (*RRMSE*)

$$RRMSE = \frac{\sqrt{\frac{1}{n}\sum_{i=1}^{n}(S_i - G_i)^2}}{\frac{1}{n}\sum_{i=1}^{n} G_i}$$

In the formula, the range of *RRMSE* is 0~∞, and there is no difference at 0.

(4) Relative Bias (*RB*)

$$RB = \frac{\sum_{i=1}^{n}(S_i - G_i)}{\sum_{i=1}^{n} G_i}$$

In the formula, the range of *RB* is −∞~+∞, and the closer to 0, the better the performance.

In these formulas, S_i represents the satellite-retrieved precipitation, and G_i represents the precipitation at the corresponding ground station. n represents the number of stations or grids, and i is a natural number ranging from 1 to n.

3. Results

As a characteristic value of precipitation, the annual maximum daily precipitation exhibits strong randomness. When evaluating the satellite-based annual maximum daily precipitation by extracting station observation data for the same period from 2000 to 2016, a total of 1675 instances of missed precipitation reports were observed, with a missed report rate of 12.5% and significant overestimation of precipitation by the satellite. On the other hand, when evaluating the satellite data by extracting station-based annual maximum daily precipitation for the same period, the underestimation of precipitation by the satellite was quite severe, with a large proportion of stations showing underestimations exceeding 30%. However, when extracting annual maximum daily precipitation for multiple years from both datasets, certain patterns emerge in the results, which will serve as the basis for further analysis in this study.

3.1. Spatial Distribution Characteristics of Satellite-Inferred Precipitation

The annual maximum daily precipitation distribution maps for each year from 2000 to 2016 obtained from the PDIR-Now satellite precipitation product are shown in Figure 2. Comparing the extreme precipitation distribution of this satellite product in China (Figure 2), it can be observed that extreme precipitation regions are primarily concentrated in the southeastern and central parts of China, with significant precipitation also frequently occurring in the northeastern regions within the study time frame. Overall, the precipitation distribution shows an increasing trend from west to east and from north to south.

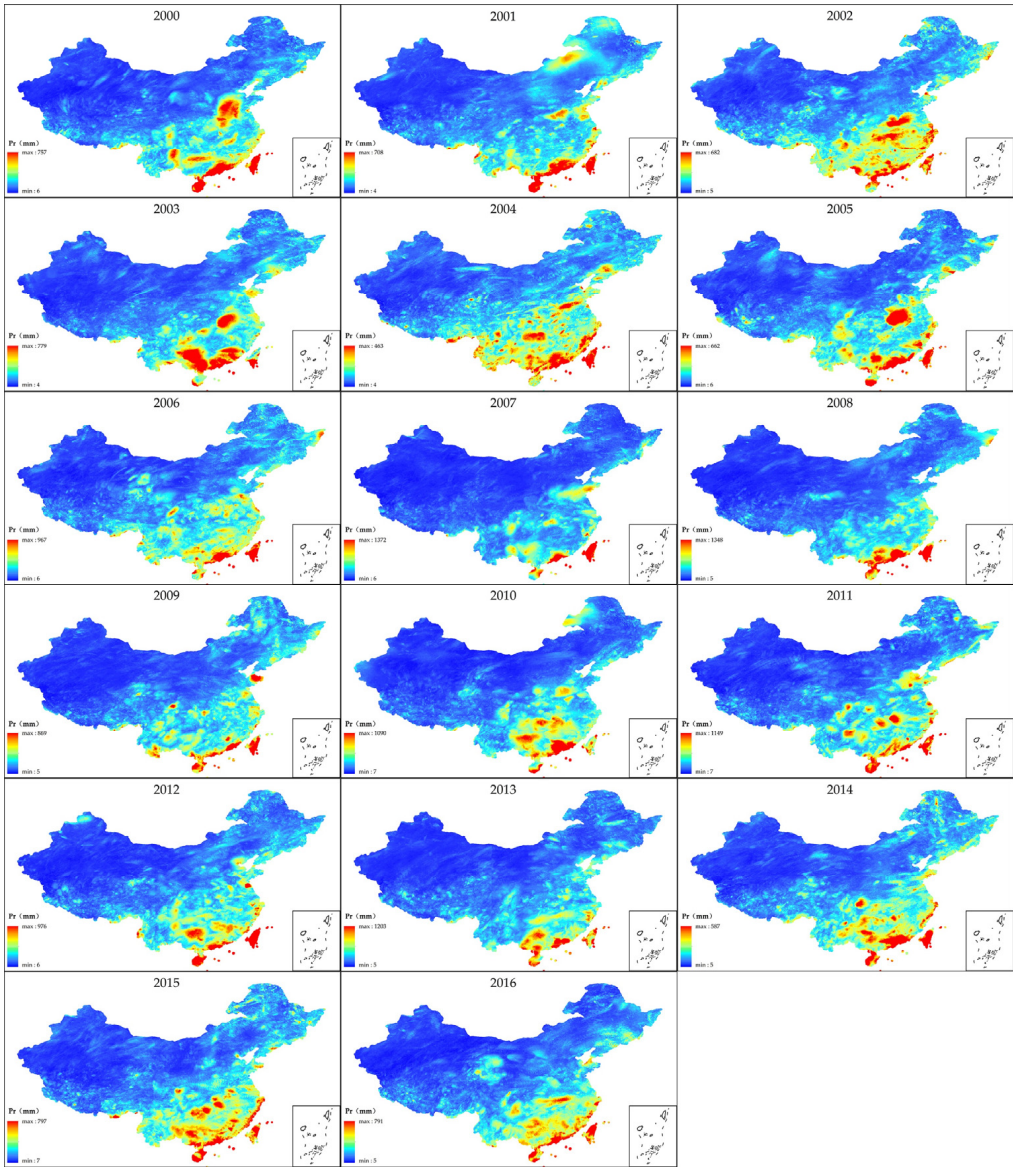

Figure 2. Annual maximum daily precipitation for satellite products from 2000 to 2016.

3.2. Overall Performance Evaluation of Satellite Data

Comparing the annual maximum daily precipitation estimated by the satellite and the station-observed data from 2000 to 2016 (17 years) at the daily scale, the overall performance of the satellite data across various metrics is quite good (Table 1). The results indicate that the PDIR-Now satellite's annual maximum daily precipitation estimates show a reasonable level of consistency with ground-based precipitation reference data, with a correlation coefficient (*R*) of 0.6, indicating a moderate correlation. The relative bias (*RB*) is −0.14; the satellite-derived annual maximum daily precipitation generally exhibits an underestimation, but there are cases where positive and negative biases cancel each other out at different stations. The root mean square error (*RMSE*) and relative root mean square error (*RRMSE*) are 46.5 mm/d and 0.6, respectively.

Table 1. Satellite inversion of precipitation assessment results.

Indicators	*R*	*RMSE*	*RRMSE*	*RB*
Result	0.6	46.5 mm/d	0.6	−0.14

3.3. Performance Evaluation of Satellite Data

3.3.1. Performance Evaluation of Different Time

The scatter plot (as shown in Figure 3) was generated by calculating the annual maximum daily precipitation retrieved from satellite data against the annually observed maximum daily precipitation at stations for the years from 2000 to 2016. The correlation coefficients (*R*) are presented in Table 2. The results show the correlation between the station-observed data (from 824 stations) and the corresponding satellite data, as well as the deviation from the measured values. In the annual data at this time scale, the correlation coefficient (*R*) generally ranges from 0.5 to 0.7 (Table 2), with 65% of the years having *R* values exceeding 0.6, indicating a moderate correlation between the two datasets. However, the inversion performance for the years 2003, 2009, 2010, and 2016 was slightly poorer, with *R* values of 0.52, 0.53, 0.54, and 0.53, respectively. The root mean square error (*RMSE*) across different years generally ranged between 40 and 60 mm. From Figure 3, it can be seen that the trend lines of all the scatter plots fall below the diagonal, indicating that the PDIR-Now satellite tends to underestimate the annual maximum daily precipitation in the study area.

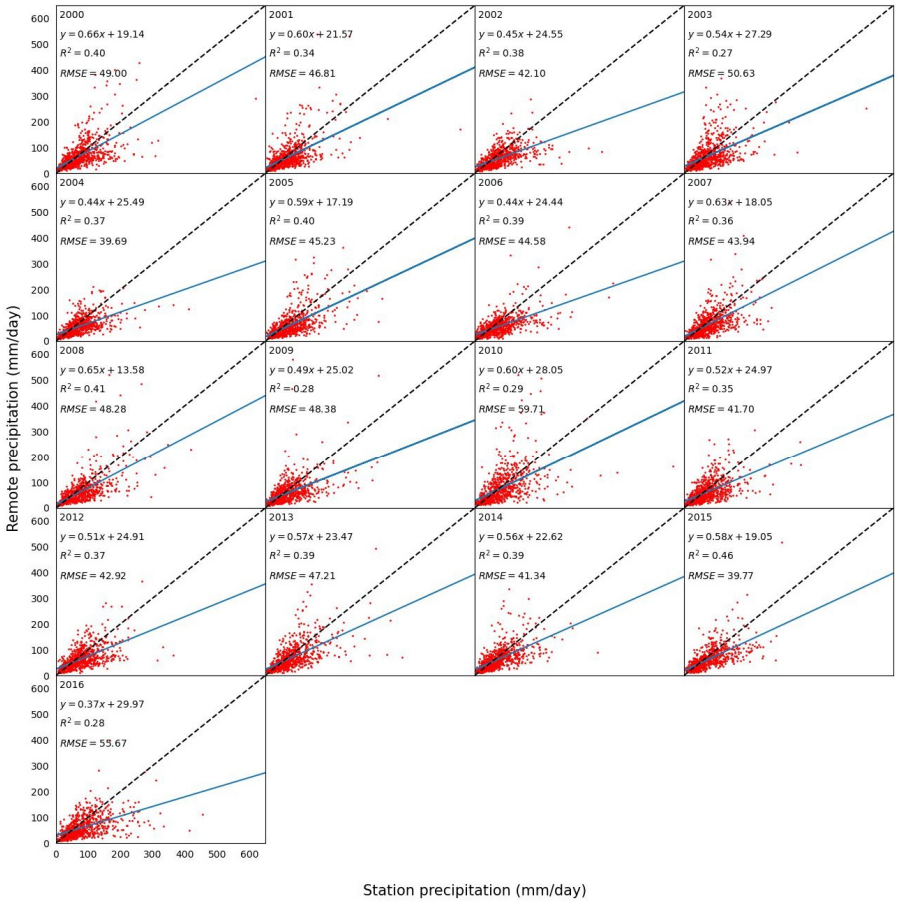

Figure 3. The distribution of annual maximum daily precipitation scatters in the study area from 2000 to 2016.

Table 2. *R* value of the study area from 2000 to 2016.

Year	2000	2001	2002	2003	2004	2005	2006	2007	2008
R	0.63	0.58	0.62	0.52	0.61	0.63	0.62	0.60	0.64
Year	2009	2010	2011	2012	2013	2014	2015	2016	
R	0.53	0.54	0.59	0.61	0.62	0.62	0.68	0.53	

3.3.2. Performance Evaluation of Different Regions

There are typically three types of evaluations when comparing satellite remote sensing precipitation with ground-based observational data: overestimation, underestimation, and agreement. Overestimation means that the selected satellite precipitation product overestimates the actual precipitation in the study area; underestimation means that the satellite product underestimates the actual precipitation; and if the error in the satellite precipitation product is within ±10% of the real precipitation, it is considered to be in agreement with the actual precipitation, referred to as "agreement" [37]. For annual maximum daily precipitation, due to the significant variation in precipitation intensity, large values, and strong randomness, it is reasonable to expand the error margin. For the study area, if the error of the annual maximum daily precipitation is within ±30%, it is considered to be in agreement with the actual precipitation. From 2000 to 2016, comparing the annual maximum daily precipitation at each station with the PDIR-Now satellite product (Figure 4), it is found that the trend of precipitation change at most stations is consistent, and the precipitation characteristics match the regional distribution patterns, validating the spatial consistency of the satellite precipitation. However, there are also some areas where significant underestimation and overestimation of precipitation occur. The stations experiencing these issues are concentrated in specific regions.

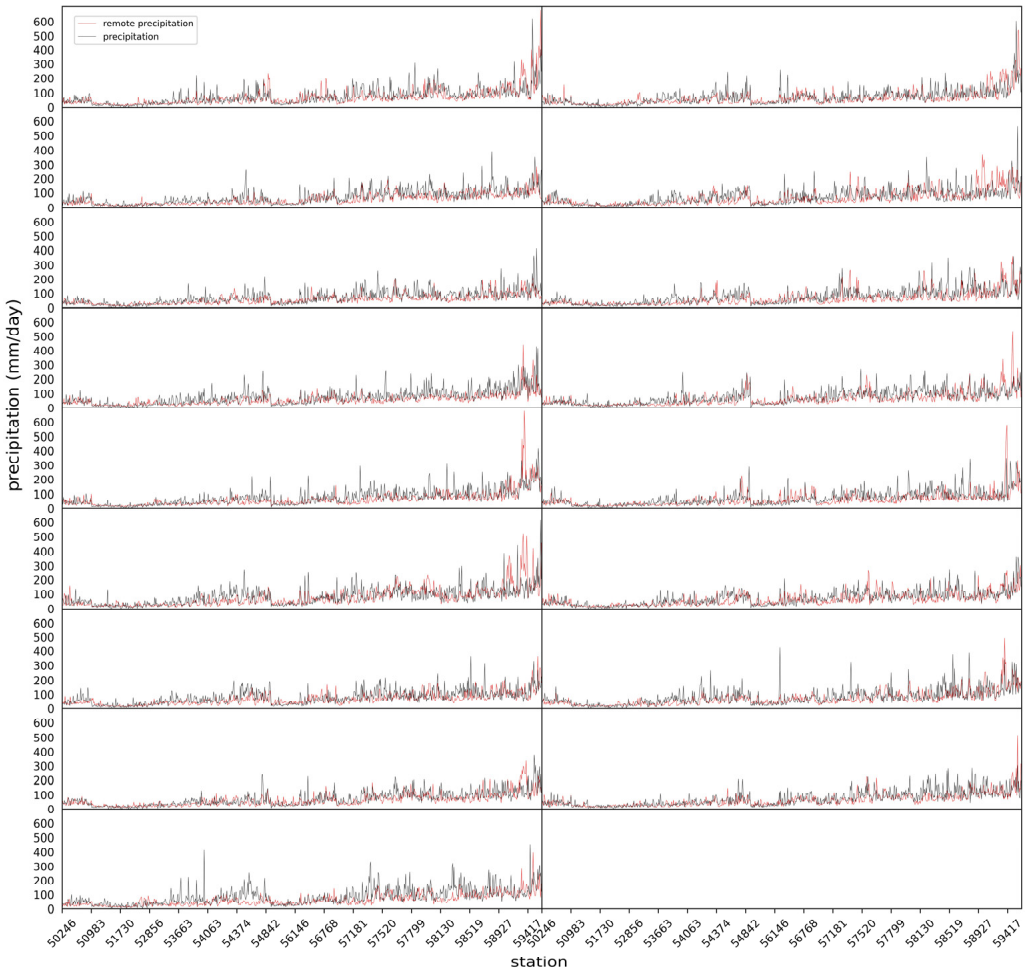

Figure 4. Comparison of annual maximum daily precipitation between stations and PDIR-Now data products in the study area from 2000 to 2016.

Further analysis of stations with larger deviations, as shown in Figure 5 and several representative years selected in Figure 6, shows that the PDIR-Now satellite product

data exhibit severe overestimation of precipitation in the northwest region, the Tibetan Plateau, and the coastal areas of southern China. Severe underestimation of precipitation is concentrated in the Loess Plateau and mostly occurs in inland areas. The relative errors at most stations are distributed between −0.3 and 0.3, with stations evenly distributed across different parts of the study area. The majority of the stations are in a state of precipitation underestimation. However, among the stations with larger errors, they are often in a state of precipitation overestimation.

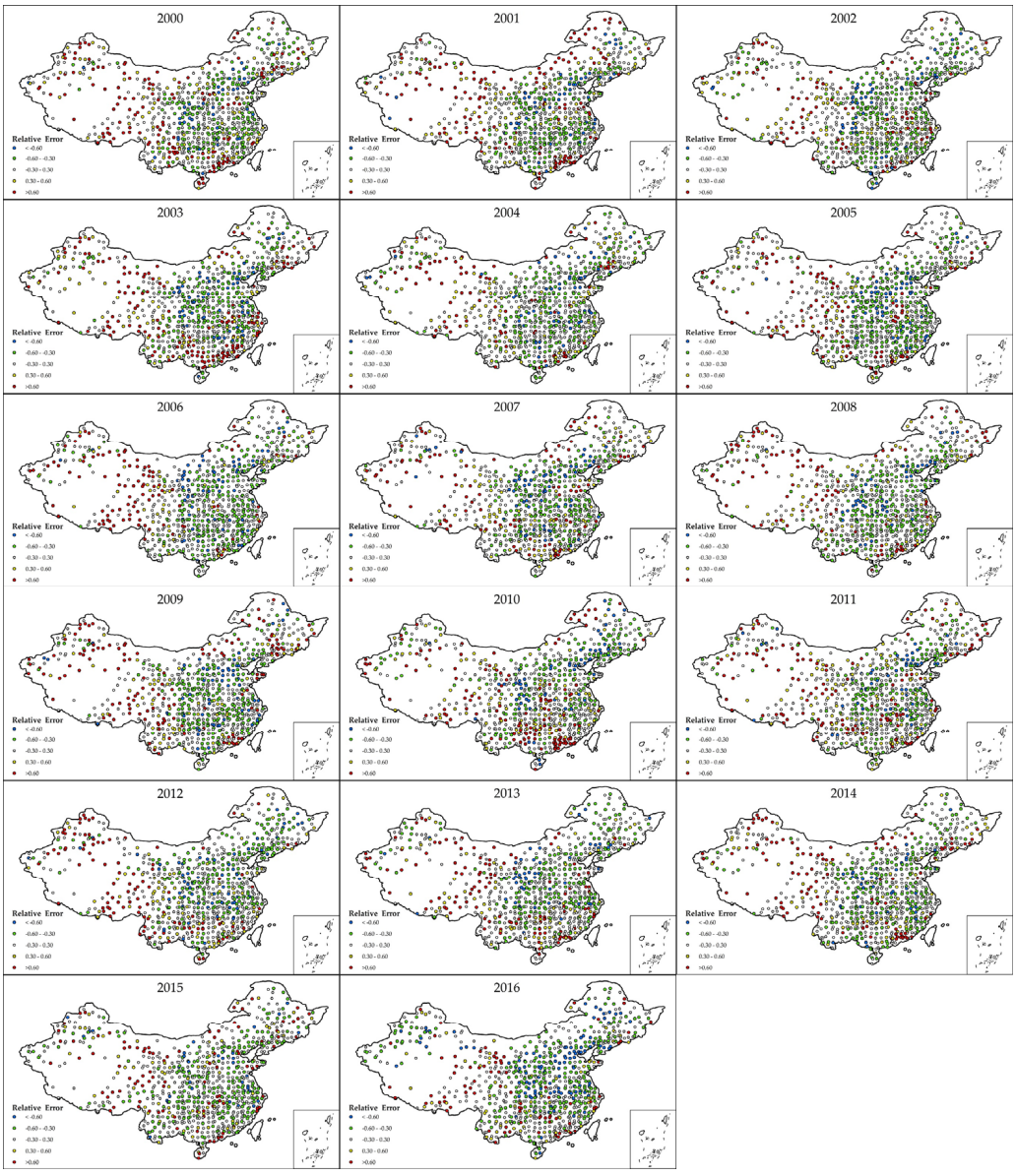

Figure 5. Spatial distribution of deviation degree of PDIR-Now data products at each site in the study area from 2000 to 2016.

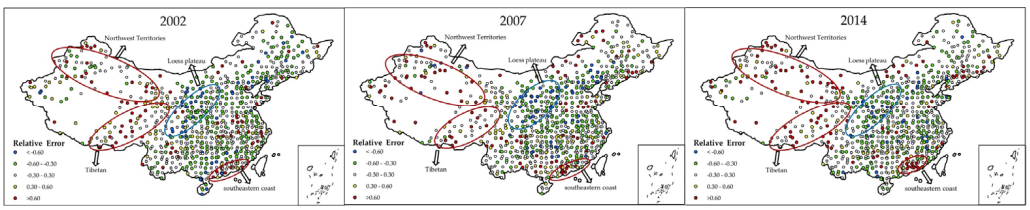

Figure 6. The relative error distribution maps for the years 2002, 2007, and 2014.

As shown in Figure 7, the distribution of the root mean square error (*RMSE*) also exhibits strong regional characteristics. The *RMSE* values in the Tibetan Plateau and Northwest regions are generally between 0 and 20 mm. In the Yunnan–Guizhou Plateau, Sichuan Basin, Northeast China, and the central part of the study area, the RMSE values range from 20 to 50 mm. In some stations along the southeastern coast, the RMSE exceeds 80 mm. In Figure 8, the relative root mean square error (*RRMSE*) more intuitively shows the spatial distribution of the deviation between the satellite data product and the observed values. The distribution of *RRMSE* values generally matches the precipitation patterns in the study area, presenting a characteristic pattern of higher values in the east and lower values in the west, with a gradual decrease from south to north. The majority of stations have *RRMSE* values between 0 and 0.6, while a smaller portion of stations have *RRMSE* values between 0.6 and 1.5. In the Northwest and Southeastern coastal areas, the *RRMSE* is generally high, and the error is large, and the *RRMSE* is even higher than 1.5 at a few sites.

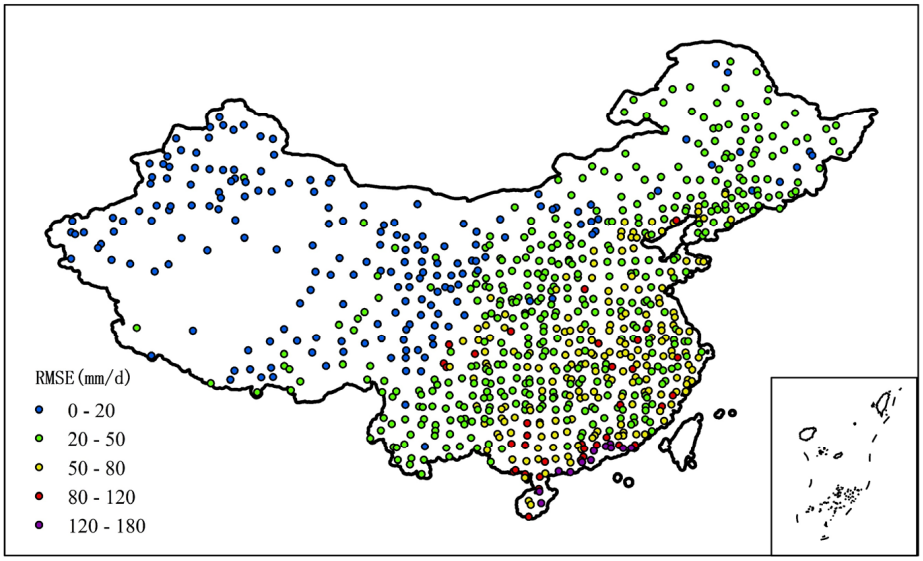

Figure 7. Spatial distribution of *RMSE* in the study area from 2000 to 2016.

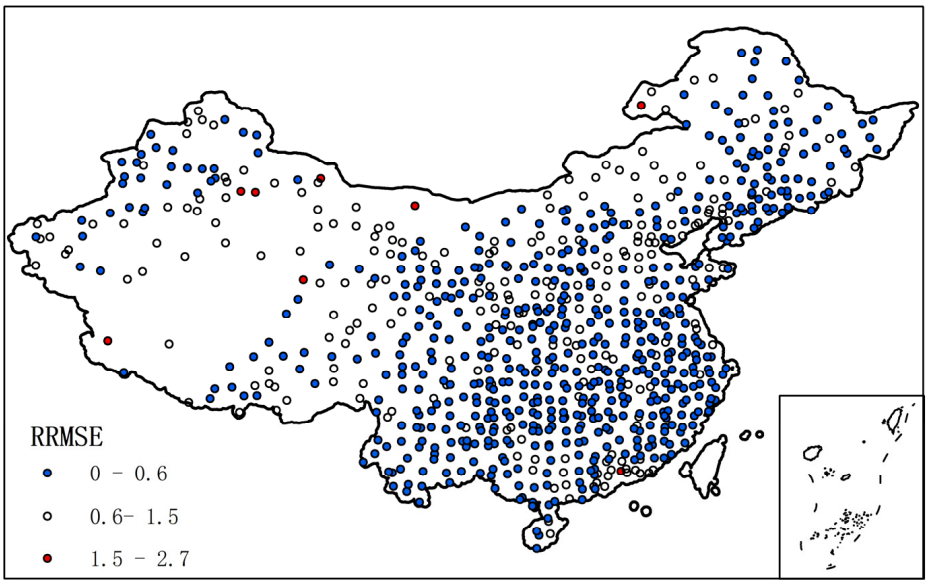

Figure 8. Spatial distribution of *RRMSE* in the study area from 2000 to 2016.

From the spatial distribution of the relative bias (*RB*) (Figure 9), it can be observed that the overall trend of the PDIR-Now satellite precipitation estimates performs well. The majority of stations have *RB* values ranging from −0.3 to 0.3. Only a small number of stations have absolute *RB* values greater than 0.7, with most of these stations located in the Northwest and Tibetan Plateau regions. Specifically, there is one station in the Inner Mongolia Autonomous Region and four stations in Guangdong Province.

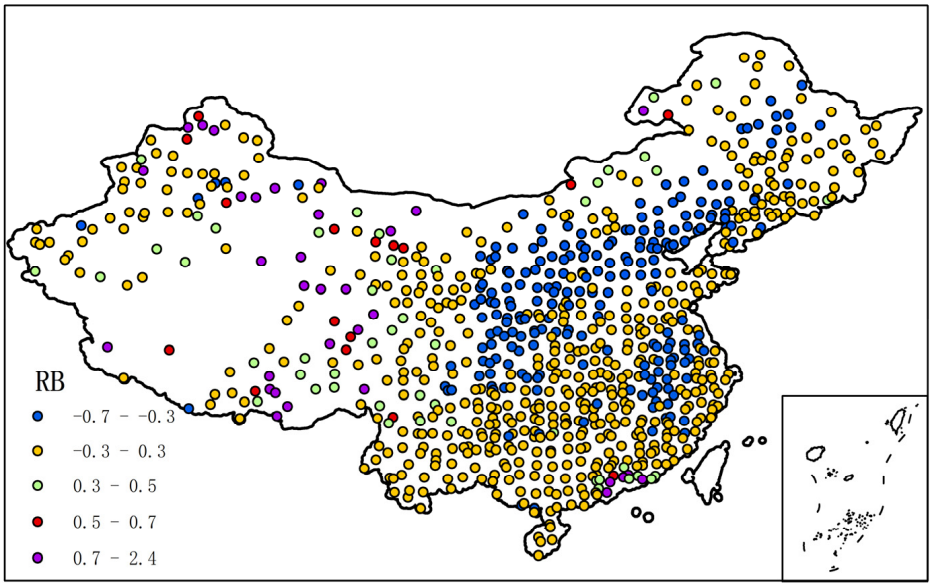

Figure 9. Spatial distribution of annual *RB* in the study area from 2000 to 2016.

4. Discussion

4.1. Impact of Nighttime Rain on Satellite Precipitation Retrieval

The study area has a large east–west and north–south span, with many plateaus, basins, and river valleys, which are prone to nighttime rainfall. In more than half of the study area, the nighttime rainfall rate exceeds 50%, with the Sichuan Basin and Tibet region even experiencing nighttime rainfall rates of over 70%. Although coastal cities are not typical nighttime rain zones, their nighttime precipitation is also significant [36,38,39]. Current satellite products like the Tropical Rainfall Measuring Mission (TRMM), Integrated Multi-satellite Retrievals for GPM (IMERG), and Global Satellite Mapping of Precipitation (GSMaP) have been found to either underestimate or overestimate rainfall in the study area. The PDIR-Now satellite data product, as a precipitation retrieval product that solely relies on IR (longwave infrared) as its input data, still faces difficulties in monitoring nocturnal rainfall despite employing high-frequency sampling of infrared imagery and increasing the cloud-top temperature threshold [32]. Furthermore, due to the complex terrain in the study area and the simple conditions for nighttime rainfall formation, the issue of monitoring nighttime rainfall still persists. Therefore, improving nighttime rainfall monitoring in this region is a critical area for further research.

4.2. Impact of Typhoons on Satellite Precipitation Retrieval

The accuracy of PDIR-Now satellite data is highly influenced by geographical factors. PDIR-Now can accurately simulate extreme precipitation patterns in the United States because it uses extensive local data correction. However, the southeastern coastal region of China, which has a tropical maritime climate and is along the primary path for typhoon development in the western Pacific, is significantly impacted by typhoons. Typhoon-induced heavy rainfall is a major contributor to extreme precipitation events in this region, characterized by high rainfall intensity, large coverage, and long duration. As seen in

Figure 9, PDIR-Now satellite data exhibit both underestimation and overestimation in precipitation monitoring for the southeastern coastal region, but the overall trend shows overestimation [40–42]. This aligns with previous studies on satellite monitoring of typhoon precipitation. However, as precipitation intensity increases, the forecast becomes more unstable, leading to a higher likelihood of false negatives, which is consistent with findings from studies on the US West Coast [32].

5. Conclusions

Based on precipitation observation data from Chinese meteorological stations, this study employs *R*, *RMSE*, *RRMSE*, and *RB* indices to comprehensively evaluate the precipitation data from the PDIR-Now satellite product. By assessing data consistency, errors, and error causes, the study investigates the satellite's ability to monitor extreme precipitation in the study area. The conclusions are as follows:

1. This study finds that, in terms of data quality, the PDIR-Now satellite products can capture the spatial distribution of extreme precipitation in the study area. In the assessment of consistency indicators, a moderate correlation is observed between the two datasets, and the assessment of annual data also shows a moderate correlation. In the assessment of error indicators, the values of *RMSE* and *RRMSE* are within an acceptable range. From the annual assessment results, the error results for 2010 and 2016 are slightly larger. The analysis attributes this to the fact that these two years were exceptionally wet in China, and due to the impact of the greenhouse effect, although the precipitation was high, the number of rainy days shortened, leading to abrupt alternations between drought and flood. While satellites can capture the occurrence of abnormal precipitation, there is often a significant deviation from the measured values at stations, with 2016 being particularly prominent as the wettest in the past 60 years. The assessment results for the other years fluctuate around the overall trend.
2. The inversion error of extreme precipitation from PDIR-Now satellite products exhibits significant regional characteristics in the study area. From the spatial distribution of data, *RMSE* increases progressively from west to east and from north to south, consistent with the spatial characteristics of precipitation. The *RRMSE*, *RB*, and relative deviation of most stations are within the normal range, but larger errors are observed in the northwest, Tibetan Plateau, and coastal areas. Stations with underestimated precipitation are mainly located in semi-arid areas such as the Loess Plateau and its surroundings, while stations with overestimated precipitation are concentrated in arid areas such as the northwest.
3. Although the annual maximum daily precipitation extracted from satellites and stations is not synchronized in time, this study reveals a relatively stable relationship between satellite and station data after analyzing the *R*, *RB*, *RMSE*, and *RRMSE* of 17 years of data from 2000 to 2016. This relationship can be applied to the estimation of rainstorm frequency curves, which is of great significance for flash flood warnings. Furthermore, based on previous research, we know that the larger the time scale, the smaller the simulation error. From the analysis of the annual maximum daily precipitation prediction results of PDIR-Now satellite products, we can infer that the prediction fitting results for 1 h intervals may have larger errors. The analysis also shows that the influence of geographical factors on satellite inversion is significant, indicating considerable room for improvement in satellite algorithms.

Author Contributions: Y.Z.: conceptualization, methodology, investigation, calculation, and writing—original draft; G.C.: formal analysis and data curation; W.Z.: resources and writing—reviewing and editing; J.G.: investigation and writing—reviewing and editing; X.L.: conceptualization, methodology, writing—reviewing and editing, and funding acquisition. All authors have read and agreed to the published version of the manuscript.

Funding: This research received no external funding.

Data Availability Statement: The meteorological data used in this study are available at the following: http://data.cma.cn, accessed on 13 January 2025. The satellite data (PDIR-Now) used in this study are available at the following: https://chrsdata.eng.uci.edu/, accessed on 13 January 2025.

Acknowledgments: The authors would like to thank the National Climatic Center of the China Meteorological Administration for providing the climate database used in this study. At the same time, we would like to thank the Center for Hydrometeorology and Remote Sensing for providing data support.

Conflicts of Interest: Author Jingyu Guo is employed by the company Sichuan China Railway Erju Engineering Group Co., Ltd. The remaining authors declare that the research was conducted in the absence of any commercial or financial relationships that could be construed as a potential conflict of interest.

References

1. Sen, Z.; Al-Harithy, S.; As-Sefry, S. Possible climate change implications for Saudi Arabian meteorology station maximum daily rainfall records. *Int. J. Glob. Warm.* **2018**, *14*, 488–509. [CrossRef]
2. Ngo-Duc, T. Rainfall Extremes in Northern Vietnam: A Comprehensive Analysis of Patterns and Trends. *Vietnam J. Earth Sci.* **2023**, *45*, 183–198. [CrossRef]
3. Alharbi, R.S.; Dao, V.; Jimenez Arellano, C.; Nguyen, P. Comprehensive Evaluation of Near-Real-Time Satellite-Based Precipitation: PDIR-Now over Saudi Arabia. *Remote Sens.* **2024**, *16*, 703. [CrossRef]
4. Hou, A.Y.; Kakar, R.K.; Neeck, S.; Azarbarzin, A.A.; Kummerow, C.D.; Kojima, M.; Oki, R.; Nakamura, K.; Iguchi, T. The Global Precipitation Measurement Mission. *Bull. Am. Meteorol. Soc.* **2014**, *95*, 701–722. [CrossRef]
5. Huffman, G.J.; Bolvin, D.T. *TRMM and Other Data Precipitation Data Set Documentation*; NASA: Greenbelt, MA, USA, 2015.
6. Joyce, R.J.; Janowiak, J.E.; Arkin, P.A.; Xie, P. CMORPH: A Method that Produces Global Precipitation Estimates from Passive Microwave and Infrared Data at High Spatial and Temporal Resolution. *J. Hydrometeorol.* **2004**, *5*, 487–503. [CrossRef]
7. Guo, B.; Xu, T.; Yang, Q.; Zhang, J.; Dai, Z.; Deng, Y.; Zou, J. Multiple Spatial and Temporal Scales Evaluation of Eight Satellite Precipitation Products in a Mountainous Catchment of South China. *Remote Sens.* **2023**, *15*, 1373. [CrossRef]
8. Navarro, A.; García-Ortega, E.; Merino, A.; Sánchez, J.L. Extreme Events of Precipitation over Complex Terrain Derived from Satellite Data for Climate Applications: An Evaluation of the Southern Slopes of the Pyrenees. *Remote Sens.* **2020**, *12*, 2171. [CrossRef]
9. Bai, L.; Shi, C.; Li, L.; Yang, Y.; Wu, J. Accuracy of CHIRPS Satellite-Rainfall Products over Mainland China. *Remote Sens.* **2018**, *10*, 362. [CrossRef]
10. Bagaglini, L.; Sanò, P.; Casella, D.; Cattani, E.; Panegrossi, G. The Passive Microwave Neural Network Precipitation Retrieval Algorithm for Climate Applications (PNPR-CLIM): Design and Verification. *Remote Sens.* **2021**, *13*, 1701. [CrossRef]
11. Huffman, G.J.; Adler, R.F.; Bolvin, D.T.; Nelkin, E.J.; Wolff, D.B.; Adler, R.F.; Gu, G.; Hong, Y.; Bowman, K.P.; Stocker, E.F. The TRMM Multisatellite Precipitation Analysis (TMPA): Quasi-Global, Multiyear, Combined-Sensor Precipitation Estimates at Fine Scales. *J. Hydrometeorol.* **2007**, *8*, 38–55. [CrossRef]
12. Skofronick-Jackson, G.; Petersen, W.A.; Berg, W.; Kidd, C.; Stocker, E.F.; Kirschbaum, D.B.; Kakar, R.; Braun, S.A.; Huffman, G.J.; Iguchi, T.; et al. The Global Precipitation Measurement (GPM) Mission for Science and Society. *Bull. Am. Meteorol. Soc.* **2017**, *98*, 1679–1695. [CrossRef]
13. Echeta, O.C.; Adjei, K.A.; Andam-Akorful, S.A.; Gyamfi, C.; Darko, D.; Odai, S.N.; Kwarteng, E.V.S. Performance Evaluation of Near-Real-Time Satellite Rainfall Estimates over Three Distinct Climatic Zones in Tropical West-Africa. *Environ. Process.* **2022**, *9*, 59. [CrossRef]
14. Gorooh, V.A.; Shearer, E.J.; Nguyen, P.; Hsu, K.; Sorooshian, S.; Cannon, F.; Ralph, M. Performance of New Near-Real-Time PERSIANN Product (PDIR-Now) for Atmospheric River Events over the Russian River Basin, California. *J. Hydrometeorol.* **2022**, *23*, 1899–1911. [CrossRef]

15. Liu, G.; Zhu, Z.; Tan, X. Evaluation of High-Resolution Remote Sensing Precipitation Products' Ability to Monitor Heavy Precipitation—A Case Study of Typhoon "Wipha" in 2014. *J. Subtrop. Resour. Environ.* **2017**, *12*, 39–48.
16. Liu, Y.; Wu, Y.; Feng, Z.; Huang, X.; Wang, D. Evaluation of Multiple Satellite Precipitation Products' Performance in Retrieving Extreme Rainfall in China. *Trop. Geogr.* **2017**, *37*, 417–433.
17. Pang, C. Evaluation of Multiple Satellite Precipitation Products' Monitoring Ability for Extreme Precipitation in Mainland China. Master's Thesis, Henan University, Zhengzhou, China, 2023.
18. Xie, W.; Yi, S.; Leng, C. Impacts of Gauge Data Bias on the Performance Evaluation of Satellite-Based Precipitation Products in the Arid Region of Northwestern China. *Water* **2022**, *14*, 1860. [CrossRef]
19. Nadarajah, S.; Choi, D. Maximum daily rainfall in South Korea. *J. Earth Syst. Sci.* **2007**, *116*, 311–320. [CrossRef]
20. García-Marín, A.P.; Ayuso-Muñoz, J.L.; Taguas-Ruiz, E.V.; Estevez, J. Regional analysis of the annual maximum daily rainfall in the province of Malaga (southern Spain) using the principal component analysis. *Water Environ. J.* **2011**, *25*, 522–531. [CrossRef]
21. Villarini, G.; Smith, J.A.; Ntelekos, A.A.; Schwarz, U. Annual maximum and peaks-over-threshold analyses of daily rainfall accumulations for Austria. *J. Geophys. Res.* **2011**, *116*, D05103. [CrossRef]
22. Donat, M.G.; Alexander, L.V.; Yang, H.; Durre, I.; Vose, R.; Dunn, R.J.H.; Willett, K.M.; Aguilar, E.; Brunet, M.; Caesar, J.; et al. Updated analyses of temperature and precipitation extreme indices since the beginning of the twentieth century: The HadEX2 dataset. *J. Geophys. Res. Atmos.* **2013**, *118*, 2098–2118. [CrossRef]
23. Porto de Carvalho, J.R.; Assad, E.D.; de Oliveira, A.F.; Pinto, H.S. Annual maximum daily rainfall trends in the Midwest, southeast and southern Brazil in the last 71 years. *Weather Clim. Extrem.* **2014**, *5–6*, 7–15. [CrossRef]
24. Wang, T.; Song, C.; Chen, X. Clarifying the relationship between annual maximum daily precipitation and climate variables by wavelet analysis. *Atmos. Res.* **2023**, *295*, 106981. [CrossRef]
25. Wang, Z.; Wilby, R.L.; Yu, D. Spatial and temporal scaling of extreme rainfall in the United Kingdom. *Int. J. Climatol.* **2024**, *44*, 286–304. [CrossRef]
26. Kong, F.; Shi, P.; Fang, J.; Lü, L.; Fang, J.; Guo, J. Research Progress and Prospects on the Temporal and Spatial Patterns of Extreme Precipitation and Its Influencing Factors under the Background of Global Change. *Disaster Sci.* **2017**, *32*, 165–174.
27. Ding, M.; Yong, B.; Yang, Z. Study on the Extreme Precipitation Monitoring Potential of the Global Precipitation Measurement (GPM) Multi-Satellite Combined Precipitation Product. *J. Remote Sens.* **2022**, *26*, 657–671.
28. Yang, X.; Zeng, S.; Lin, Z. Evaluation of GPM Satellite Precipitation Data for Monitoring Extreme Precipitation in Sichuan. *Remote Sens. Technol. Appl.* **2023**, *38*, 1496–1508.
29. Shang, M.; Ren, Y.; Song, H.; Yao, Y.; Bai, L.; Li, Y.; Ma, J. Evaluation of IMERG and GSMaP for Monitoring Extreme Precipitation in China. *J. Earth Inf. Sci.* **2023**, *25*, 1813–1826.
30. Liu, R.; Jiang, S.; Ren, L.; Wei, L.; Wang, M.; Lu, Y. Evaluation of IMERG Precipitation Product from the Global Precipitation Measurement (GPM) Mission for Monitoring Extreme Rainfall in Mainland China. *China Rural Water Resour. Hydropower* **2021**, *4*, 57–63.
31. Yu, J.; Shen, Y.; Pan, Y.; Xiong, A. Comparative Evaluation of China's Regional Daily Merged Precipitation Dataset and International Precipitation Products. *Acta Meteorol. Sin.* **2015**, *73*, 394–410.
32. Nguyen, P.; Shearer, E.J.; Ombadi, M.; Gorooh, V.A.; Hsu, K.; Sorooshian, S.; Logan, W.S.; Ralph, M. PERSIANN Dynamic Infrared–Rain Rate Model (PDIR) for High-Resolution, Real-Time Satellite Precipitation Estimation. *Bull. Am. Meteorol. Soc.* **2020**, *101*, E286–E302. [CrossRef]
33. Jimenez Arellano, C.; Dao, V.; Afzali Gorooh, V.; Alharbi, R.S.; Nguyen, P. Performance of the PERSIANN Family of Products over the Mekong River Basin and Their Application for the Analysis of Trends in Extreme Precipitation Indices. *Atmosphere* **2023**, *14*, 1832. [CrossRef]
34. Dong, Y.; Gan, F.; Gao, Y.; Diao, X.; Pan, Y. Evaluation of IMERG Satellite Precipitation Data for Drought Monitoring in the Jialing River Basin. *Hydrology* **2023**, *43*, 88–95.
35. Huang, W.R.; Liu, P.Y.; Hsu, J. Multiple timescale assessment of wet season precipitation estimation over Taiwan using the PERSIANN family products. *Int. J. Appl. Earth Obs. Geoinf.* **2021**, *103*, 102521. [CrossRef]
36. Ma, Q.; Li, Y.; Feng, H.; Yu, Q.; Zou, Y.; Liu, F.; Pulatov, B. Performance evaluation and correction of precipitation data using the 20-year IMERG and TMPA precipitation products in diverse subregions of China. *Atmos. Res.* **2021**, *249*, 105304. [CrossRef]
37. Wang, Z.; Shi, Y.; Zhang, T. Does TRMM Satellite Precipitation Underestimate or Overestimate Precipitation in Mainland China? *Adv. Earth Sci.* **2021**, *36*, 604–615.
38. Zhou, Z.; Guo, B.; Xing, W.; Zhou, J.; Xu, F.; Xu, Y. Comprehensive evaluation of latest GPM era IMERG and GSMaP precipitation products over mainland China. *Atmos. Res.* **2020**, *246*, 105132. [CrossRef]
39. Zhao, T.; Yatagai, A. Evaluation of TRMM 3B42 product using a new gauge-based analysis of daily precipitation over China: Evaluation of TRMM 3B42 Product over China. *Int. J. Climatol.* **2014**, *34*, 2749–2762. [CrossRef]

40. Han, F.; Lu, X.; Wu, T.; Xu, Y.; Han, X.; Cai, X. Evaluation of Multi-Satellite Merged Precipitation Products for Monitoring Typhoon Precipitation in Zhejiang Province from 2015 to 2020. *Rainstorm Disasters* **2023**, *42*, 57–66.
41. Ehsani, M.R.; Heflin, S.; Risanto, C.B.; Behrangi, A. How well do satellite and reanalysis precipitation products capture North American monsoon season in Arizona and New Mexico? *Weather Clim. Extrem.* **2022**, *38*, 100521. [CrossRef]
42. Huang, W.R.; Liu, P.Y.; Chang, Y.H.; Lee, C.-A. Evaluation of IMERG Level-3 Products in Depicting the July to October Rainfall over Taiwan: Typhoon Versus Non-Typhoon. *Remote Sens.* **2021**, *13*, 622. [CrossRef]